

Elongational Flow of Polymer Melts

JAMES F. STEVENSON

Chemical Engineering Department
University of Wisconsin, Madison, Wisconsin 53706

Elongational flow experiments with viscous polymeric materials were conducted at a constant elongation rate on a modified tensile testing machine. Steady elongational and shear viscosity data and elongational stress growth data are presented for an isobutylene-isoprene copolymer at 100°C. S-shaped elongational stress growth curves are reported for cis-1,4-polyisoprene at 80°C.

The stresses necessary to maintain a cylindrical specimen in steady elongational flow are indicated by a calculation which includes the effects of inertia, gravity, and interfacial tension.

Interrelations among several elongational flow material functions are given for a constitutive equation based on the theory of linear viscoelasticity.

SCOPE

A great deal of effort has been devoted to the study of polymeric materials in shear flow, but until recently relatively little research has been done on these materials in elongational flow. This lack of research may be attributed more to the relative difficulty of conducting large-strain elongational flow experiments than to their lack of relevance. To the process engineer, elongational flow and the related flow, biaxial elongation, are of interest because

they occur in such industrial processes as spinning, extrusion take-off, vacuum forming, and convergent flow in a die entry. Elongational flow data provide the theoretician with a discriminating new test for models and theories.

This paper presents the experimental techniques and results for elongational flow experiments conducted with two high viscosity polymeric materials at a constant elongation rate.

CONCLUSIONS AND SIGNIFICANCE

In a series of elongational flow experiments with two high-viscosity polymeric materials, tapered cylindrical specimens were stretched at a constant elongation rate on a modified tensile testing machine.

For an isobutylene-isoprene copolymer at 100°C. the steady elongational viscosity is equal to three times the zero-shear-rate viscosity at all experimental elongation rates. For this material the elongational stress as a function of time apparently increases monotonically to a steady state value.

The elongational stress-strain curves for cis-1,4-poly-

isoprene at 80°C. are S-shaped and, therefore the steady state elongational viscosity does not exist.

Both of the types of behavior described above have been observed by other investigators for various materials.

A solution of the stress equations of motion for elongational flow shows that the effects of gravity, inertia, and interfacial tension are negligible in the experiments conducted by the author.

A series of interrelations among elongational flow material functions based on the theory of linear viscoelasticity suggests possible correlations for experimental data and limiting predictions for models.

TERMINOLOGY

Typical relations between elongational stress and strain rate are outlined in Figure 1 for elongation experiments characterized by constant elongation rate, constant elongational stress, and a small instantaneous elongational strain.

In a constant elongation rate experiment the steady elongational viscosity ($\dot{\eta}$) is given by

$$\dot{\eta}(\dot{\gamma}) = - \frac{(\pi_{zz} - \pi_{rr})}{\dot{\gamma}} \quad (1)$$

where π_{zz} and π_{rr} are the steady state axial and radial components of the total stress that are necessary to stretch a cylindrical specimen at a constant elongation rate. The difference $\pi_{zz} - \pi_{rr}$ is dependent on the elongation rate.

As shown by a calculation in Appendix A, when the effects of gravity, inertia, and interfacial tension are considered, the steady state values of the stresses π_{zz} and π_{rr} individually vary with the coordinates z and r , the radius of the specimen R and the elongation rate $\dot{\gamma}$. Ideally, to

J. F. Stevenson is with the School of Chemical Engineering, Cornell University, Ithaca, New York 14850.

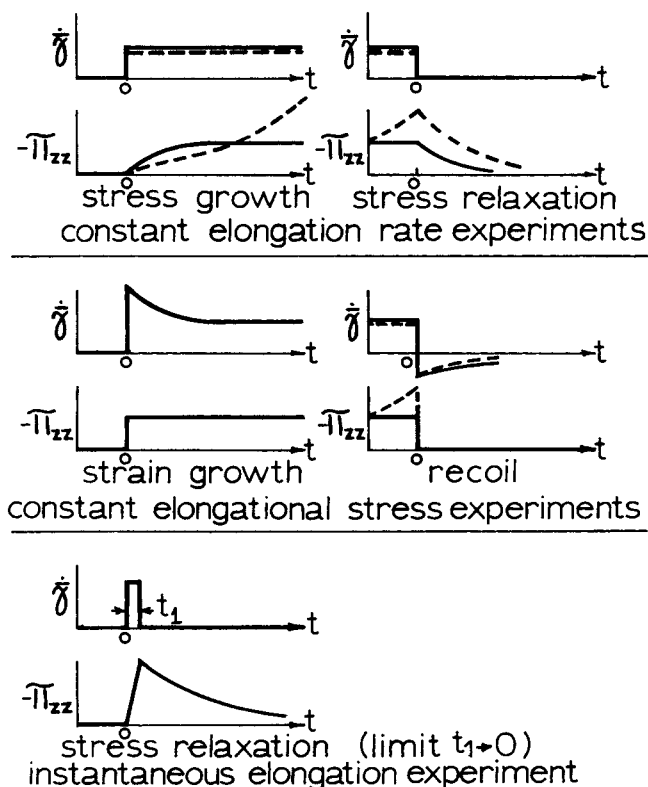


Fig. 1. Elongational flow experiments characterized by constant elongation rate at $t > 0$, constant elongational stress at $t > 0$, and instantaneous elongation. The behavior of materials for which the elongational stress-strain curve attains steady state in constant elongation rate experiments is shown by (—) whereas the behavior of materials with an S-shaped elongational stress-strain curve in constant elongation rate experiments is shown by (---).

maintain a cylindrical specimen in steady elongational flow it is necessary to provide along the cylindrical boundary an external radial normal stress which has a nonlinear dependence on z and R . But in an experiment the only external radial normal stress that can be applied to the specimen π_{rr}^e is the hydrostatic pressure which varies linearly with the z coordinate. However, as shown in Appendix A for experiments conducted with high viscosity polymers immersed in a liquid of comparable density, the difference between the radial normal stress necessary to maintain elongational flow π_{rr} and the experimentally applicable radial normal stress π_{rr}^e is small compared to the elongational stress $\pi_{zz} - \pi_{rr}^e$. Similarly, during elongational stress growth experiments the difference between the radial normal stresses π_{rrG} and π_{rr}^e is small compared to the elongational stress during stress growth $\pi_{zzG} - \pi_{rr}^e$ except at the low stress levels at the beginning of the experiment.

The stresses which can be applied experimentally therefore are sufficient to stretch the specimen at an elongation rate that is very nearly constant along the monitored portion of the specimen. Furthermore, the contributions of gravity, inertia, and interfacial tension to the measured tensile force are so small in the monitored portion of the specimen that they can be neglected in the calculation of the elongational stress and elongational viscosity.

In the remainder of this paper with the exception of Appendix A the term $\pi_{zzG} - \pi_{rrG}$ will be referred to as $\pi_{zzG}(\dot{\gamma}, t)$.

The total elongational strain at the end of a constant elongation rate experiment $\bar{\gamma}_m$ can be divided into a recoverable component $\bar{\gamma}_r$ and an irrecoverable component $\bar{\gamma}_i$. The values of these strains are given by

$$\bar{\gamma}_m = \ln(L_m/L_0) \quad (2)$$

$$\bar{\gamma}_i = \ln(L_i/L_0) \quad (3)$$

$$\bar{\gamma}_r = \bar{\gamma}_m - \bar{\gamma}_i = \ln(L_m/L_i) \quad (4)$$

where L_0 is the initial length of the monitored section of the specimen. L_m is its maximum strained length, and L_i is its final length after recoil. During a constant elongation rate experiment, the length of the specimen L and the total elongational strain $\bar{\gamma}$ vary with time in the following manner:

$$L = L_0 \exp(\dot{\gamma} t) \quad (5)$$

$$\bar{\gamma} = \dot{\gamma} t \quad (6)$$

In the constant elongation stress experiment, a constant stress π_{zz0} is applied to the specimen and the elongational strain is monitored. For this type of experiment Cogswell (2) defined the elastic strain γ_e as the intercept obtained by extrapolating the linear portion of the elongational strain versus time curve to zero time.

In the third type of experiment the relaxing stress $\pi_{zz}(\epsilon, t)$ is measured following a small, elongational strain of magnitude ϵ applied over a short time interval t_1 . The data from this experiment are usually reported as relaxation modulus $E_r(t)$ (3) versus time where

$$E_r(t) = \frac{-\pi_{zz}(\epsilon, t)}{\epsilon} \quad (\text{small } \epsilon) \quad (7)$$

and

$$\epsilon = \frac{L_m - L_0}{L_0} \simeq \bar{\gamma}_m \quad (\text{small } \epsilon) \quad (8)$$

A constitutive equation based on the theory of linear viscoelasticity gives the following relation among the material functions discussed in this section.

$$\frac{\int_0^\infty (\pi_{zz}(\dot{\gamma}) - \pi_{zzG}(\dot{\gamma}, t)) dt}{\pi_{zz}(\dot{\gamma})} = \frac{\bar{\gamma}_r}{\dot{\gamma}} = \frac{\bar{\gamma}_e}{\dot{\gamma}} = \frac{\int_0^\infty E_r(t) t dt}{\int_0^\infty E_r(t) dt} \quad (9)$$

This relation is derived in Appendix B and is valid in the limit as $\lambda_1 \dot{\gamma}$ and ϵ approach zero where λ_1 is the longest relaxation time for the fluid.

PREVIOUS EXPERIMENTAL WORK

Ballman (4) in 1965 measured the elongational viscosity of atactic polystyrene melt in a series of constant elongation rate experiments. Table 1 gives a summary of the experimental results obtained by Ballman and the other investigators mentioned below.

Vinogradov and co-workers (5 to 8) have measured the elongational viscosity and recoverable and irrecoverable components of the elongational strain for polyisobutylene and atactic polystyrene. For the atactic polystyrene they also obtained stress relaxation versus time curves for various values of $\bar{\gamma}_m$. In their experiments the specimen, an extruded rod which floated on a liquid bath, was elongated at a constant elongation rate by a testing machine controlled by an electronic programming device.

At low elongation rates the elongational viscosity for both polyisobutylene and atactic polystyrene was reported to be equal to three times the zero-shear-rate viscosity. At the highest elongation rates investigated for polyisobutylene at 22°C. and for intermediate elongation rates

for polystyrene, the elongational viscosity was reported to increase with increasing elongation rate. At the highest elongation rates investigated for polystyrene the elongational stress did not attain a steady state value.

For polyisobutylene the recoverable strain increased monotonically with time to a steady state value at all elongation rates for which data were reported, but for polystyrene the recoverable strain attained a steady state value only at low elongation rates.

Meissner (9, 10) has constructed a novel extensional rheometer and measured the elongational viscosity and recoverable strain of low density polyethylene. In Meissner's experiment, the specimen was clamped between two pairs of gears which rotated at a constant angular velocity. The portion of the specimen remaining between the two pairs of gears was stretched at a constant elongation rate.

Meissner reported that the elongational stress-strain curves for low density polyethylene are S-shaped for elongation rates ranging from 1 s^{-1} down to at least 0.002 s^{-1} . By plotting the elongational viscosity during stress growth $\bar{\eta}_G(\bar{\gamma}, t)$ versus time, Meissner demonstrated that for a total elongational strain $\bar{\gamma} < 1$, the elongational viscosity data for various elongation rates superpose and that the superposed elongational viscosity data nearly coincide with a curve representing three times the shear viscosity during shear stress growth at low shear rates.

Cogswell (2, 11) has constructed a constant stress rheometer to carry out elongational flow experiments under the condition of constant elongational stress. In a constant stress experiment with materials which ultimately attain steady state flow conditions, the total elongational strain initially increases rapidly with time but eventually

TABLE 1. SUMMARY OF ELONGATIONAL VISCOSITY DATA

Investigator & references	Material/ molecular weight	Tempera- ture, °C.	Zero- shear-rate viscosity, poise	$\frac{\bar{\eta}_0}{\eta_0}$	Behavior of elongational viscosity			Behavior of recoverable strain		
					SVC	SVD	SVPL	SVC	SVD	SVPL
Ballman (4)	atactic polystyrene $M_v = 3.2 \times 10^5$ $M_n = 1.3 \times 10^5$	149	—	—	—	C ¹	—	—	—	—
Radushkevich, Fikhman, & Vinogradov (5 to 8)	polyisobutylene $M_v = 7.0 \times 10^4$	22	1.0×10^7	3.16	C	C	I	S	S	—
		40	2.8×10^6	2.76	C	C	—	—	—	—
		60	$\sim 7.3 \times 10^5$	3.03	C	C	—	—	—	—
Meissner (9, 10)	atactic polystyrene $M_v = 3.0 \times 10^5$	130	$\sim 8 \times 10^7$	~ 3	C	I-U	U	S	S-U	—
	low density polyethylene $M_w = 4.8 \times 10^5$ $M_n = 1.7 \times 10^4$	150	5.0×10^5	—	²	U	U ³	U	U	3,4
Cogswell (2, 11)	polymethyl- methacrylate	190	1.0×10^6	3.2	C	⁵	—	—	—	—
	low density polyethylene	130	5.0×10^6	2.6	—	I	5	—	—	—
Stevenson (13)	polyisobutylene-	80	3.8×10^7	2.84	C	C	—	—	—	—
	isoprene copolymer	100	8.0×10^6	2.91	C	C	—	—	—	—
	$M_v = 3.5 \times 10^5$ cis-1,4-polyisoprene	80	$\sim 10^8$	—	U (no shear viscosity data)			—	—	—

1. Since the reported strain rates for elongational viscosity data and shear viscosity data did not overlap, this result is based on a reasonable extrapolation of the shear viscosity data.

2. At the lowest experimental elongation rate, the elongational viscosity apparently attained a time-independent value, but the recoverable elongational strain was still time-dependent.

3. Since a complete shear viscosity curve was not reported, it is not possible to be certain that the highest elongation rates are in the SVPL group.

4. At the highest experimental elongation rates, the recoverable strain approached a time-independent value, but the elongational stress was time-dependent and ultimately began to decrease with increasing time (or strain).

5. A convergent flow experiment which required many questionable assumptions in the data analysis showed that the elongational viscosity is independent of elongation rate in this elongation rate group.

This table gives a qualitative comparison of elongational flow behavior for several materials by referring the behavior of the material in elongational flow to its behavior in shear flow.

For the purposes of this comparison, shear rates are divided into three groups characterized by the behavior of the shear viscosity. These groups are designated: SVC (shear viscosity constant), shear rates at which the shear viscosity is constant; SVD (shear viscosity decreasing), shear rates at which the shear viscosity is decreasing but not yet in the power-law region; and SVPL (power-law shear viscosity), shear rates in the power-law region.

The behavior of the elongational viscosity versus elongation rate curve is determined for three groups of elongation rates which correspond in numerical value to the three shear rate groups. The behavior of the elongational viscosity curve for each group of elongation rates can be approximately characterized as: C (constant), elongational viscosity independent of elongation rate; I (increasing), elongational viscosity increases with increasing elongation rate; D (decreasing), elongational viscosity decreases with increasing elongation rate; or U (unsteady), elongational viscosity during stress growth is not approaching steady state at the maximum experimental strain.

The recoverable elongational strain $\bar{\gamma}_r$ versus total elongational strain $\bar{\gamma}$ curve for a group of elongation rates can generally be characterized as: S (steady), recoverable elongational strain attains a steady state value; or U (unsteady), recoverable elongational strain does not attain a steady state value.

increases linearly with time at a rate equal to the elongation rate.

The results of the constant stress rheometer experiments indicate that the elongational viscosity for polymethylmethacrylate at 190°C. is constant up to elongational stresses equal in magnitude to shear stresses for which the shear viscosity is decreasing. For low density polyethylene at 130°C. Cogswell reported that the elongational viscosity increases with increasing elongational stress at stresses which are comparable in magnitude to shear stresses at which the shear viscosity is decreasing.

Although Meissner and Cogswell worked at different temperatures and probably with different molecular weight samples of low density polyethylene, it should be noted that they reported two distinctly different types of behavior for this material in elongational flow.

EXPERIMENTAL MATERIALS, APPARATUS, AND PROCEDURES

The properties of the materials used in the elongation experiments described in this section are summarized in Table 1 under Stevenson's experiments. The isobutylene-isoprene copolymer is Butyl 035 which is made by the Enjay Chemical Company. Its composition is about 97 mole % isobutylene and 3 mole % isoprene. The cis-1,4-polyisoprene polymer is Natsyn 410 and is made by the Goodyear Tire and Rubber Company.

A schematic diagram of the elongational flow equipment is given in Figure 2. In the course of an experiment, the specimen was placed inside the constant temperature chamber which was then mounted on a variable speed testing machine. The testing machine was controlled by an analog computer. A light jewelry chain connected the specimen to the load cell which recorded the force necessary to elongate the specimen. During an experiment the length of the monitored portion of the specimen was recorded by a 35 mm camera. The force and specimen length data as functions of time were then analyzed to give the elongational stress as a function of time.

The experimental specimens were prepared in tapered plastic molds provided by the Thiokol Chemical Company (12) and especially modified for large-strain elongation experiments. The modified molds produced a specimen 9 cm in length which tapered from a diameter of 1.75 cm on the ends to a region with a constant diameter of 1.33 cm in the central portion of the specimen. The ends of the polymer specimen naturally adhered to hard rubber faucet washers which were used to attach the specimen to the equipment. The strain in the specimen was monitored by photographically recording the displacement between 5-mm wide grid marks which were made by a felt tip pen and placed 5 mm apart in the central portion

of the specimen. Shorter specimens 6 cm in length were used for the high elongation rate experiments in order to increase the maximum strain experimentally attainable.

Minimizing temperature variations around the specimen was accomplished by immersing the specimen in a stirred silicone oil bath situated inside the constant temperature chamber. The base of the specimen holder contained a mechanical stirrer which when rotated at 1100 rev./min. reduced the vertical temperature gradient within the silicone oil bath to less than 0.1°C. Inside the constant temperature chamber, air was heated by an adjustable 500 W continuous heater and a 100 W intermittent heater and was circulated around the silicone oil bath by a 150 W squirrel cage blower. Since the silicone oil and the polymer specimen were nearly the same density, the effect of gravity on the experiment was very small.

The voltage output from the analog computer was determined so that the monitored section of the specimen elongated at a constant elongation rate. The form of the voltage function was determined experimentally to be

$$E(t) = E_0 \left[\frac{t}{R_1 C_1} + \frac{t^2}{2R_1 C_1 R_2 C_2} \right] \quad (10)$$

where E is the voltage, t is the time, E_0 is the initial voltage, and R_i and C_i are the resistance and capacitance connected to the i th amplifier. The values of E_0 and of the ratio $R_1 C_1 / R_2 C_2$ depend on the size of the specimen and the elongation rate.

The elongation experiments were carried out on a MB model TM6 Universal Testing Machine made by MB Electronics, Tectron Electronics, Inc., New Haven, Conn. The hydraulically driven movable table on the machine was controlled by a closed loop servo system and had a maximum displacement of 30 cm.

The tensile force necessary to strain the specimen at a constant elongation rate was measured by a Statham Universal Transducing Cell and Load Cell Assembly.

The shear viscosity results were obtained on a Model R-16 Weissenberg Rheogoniometer made by Farol Research Engineers, Ltd., Bognor Regis, England. For work with polymer melts, the minimum shear rate obtainable was reduced to $8.52 \times 10^{-6} \text{ s}^{-1}$ by replacing the 1,800 rev./min. synchronous motor with a variable speed motor set to operate at 18 rev./min. Temperature control on the Rheogoniometer was improved by replacing the standard on-off controller with a VersaTherm Model 2156 Proportional Electronic Controller. The experimental equipment is described in greater detail elsewhere (13).

EXPERIMENTAL RESULTS

For a constant elongation rate experiment the measured values of the tensile force and the length of the monitored section of the specimen (the 5 mm section between grid marks) as functions of time were analyzed in the following way:

1. The elongation rate was defined as the slope of a least-mean square fit of the logarithm of the monitored section length versus time curve. In certain experiments, measurements of the monitored section length deviated from constant elongation rate conditions at low strains. These measurements were deleted from the analysis to avoid biasing the steady state results at large strains.

2. Small corrections for the specimen weight and thermal expansion were applied to the tensile force measurements which were then divided by the cross-sectional area to give the elongational stress during stress growth $\pi_{zz}(\bar{\gamma}, t)$. The volume of the specimen was assumed to be constant.

The steady elongational viscosity $\bar{\eta}(\bar{\gamma})$ was calculated by dividing the steady state elongational stress $\pi_{zz}(\bar{\gamma})$ by the elongation rate.

$$\bar{\eta}(\bar{\gamma}) = \frac{-\pi_{zz}(\bar{\gamma})}{\dot{\bar{\gamma}}} \quad (11)$$

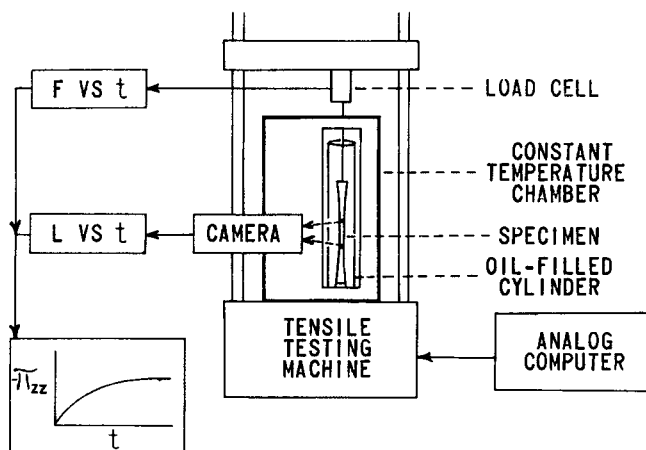


Fig. 2. Schematic diagram of elongational flow apparatus.

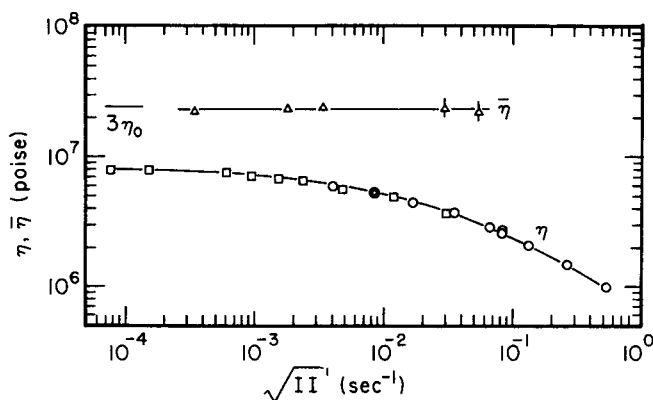


Fig. 3. Steady elongational and shear viscosity data for Butyl 035 at 100°C. The ordinate is the square root of the second invariant of the rate-of-strain tensor. Δ Elongational viscosity; \triangle Elongational viscosity (extrapolated elongational stress); \square Shear viscosity (steady shear experiment); \circ Shear viscosity (oscillatory experiment).

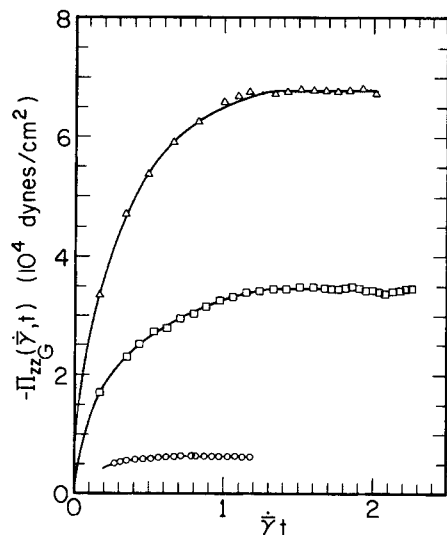


Fig. 4. Elongational stress versus strain for Butyl 035 at 100°C. (low elongation rates). Symbols represent elongation rates as indicated: \circ 2.85×10^{-4} s $^{-1}$; \square 1.48×10^{-3} s $^{-1}$; \triangle 2.82×10^{-3} s $^{-1}$. Note that the elongational stress attains steady state.

The steady shear viscosity data at the higher shear rates were obtained from complex shear viscosity data by use of the Cox-Merz (14) empirical relation

$$\eta(\dot{\gamma}) = |\eta^*(\omega)|_{\omega=\dot{\gamma}} \quad (12)$$

where η^* is the complex shear viscosity.

In Figure 3 the steady elongational and steady shear viscosity for Butyl 035 at 100°C. are graphed as functions of the square root of the second invariant of the rate of strain tensor. The second invariant of the rate-of-strain tensor II is defined as

$$II = \dot{\gamma} : \dot{\gamma} \quad (13)$$

where $\dot{\gamma}$ is the rate-of-strain tensor. For shear flow $II = \dot{\gamma}^2/2$ and for elongational flow $II = 3\dot{\gamma}^2/2$.

The two steady elongational viscosity data points marked with a vertical slash in Figure 3 were obtained by a short extrapolation of the two lower elongational stress growth curves shown in Figure 5. The values of the steady state elongational stress obtained by this procedure were

never more than 3.5% greater than the maximum value of the measured elongational stress. This extrapolation procedure is based on the assumption that the elongational stress monotonically approaches a steady state value. Support for this assumption is given by Vinogradov, Radushkevich, and Fikhman's (5) data for a similar material which show that both the elongational stress and the recoverable component of the elongational strain increase monotonically to steady state values.

Elongational stress versus strain curves for Butyl 035 at 100°C. are shown in Figures 4 and 5. Figure 6 shows the elongational stress versus strain curve for Natsyn 410 at 80°C. At the elongation rates used in this research, the elongational stress growth data for Butyl 035 and Natsyn 410 are fundamentally different. The elongational stress-strain data for Butyl 035 approach steady state values at large strains whereas for Natsyn 410 the data fall on an S-shaped curve.

In Figures 4, 5, and 6 the data points at low strains on some of the curves were omitted because of irregularities in the elongation rate at the beginning of the experiment.

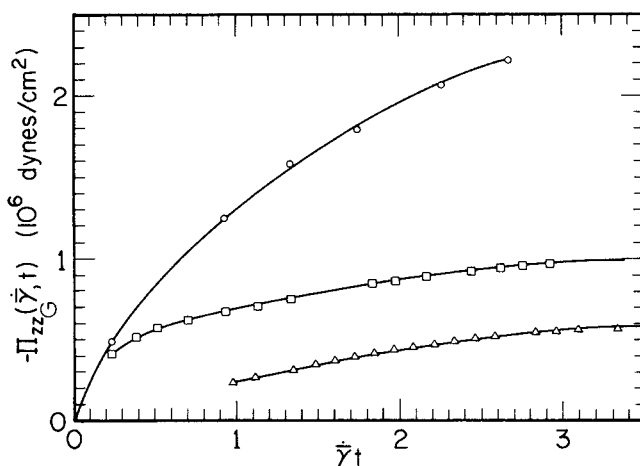


Fig. 5. Elongational stress versus strain for Butyl 035 at 100°C. (high elongation rates). Symbols represent elongation rates as indicated: \triangle 2.48×10^{-2} s $^{-1}$; \square 4.51×10^{-2} s $^{-1}$; \circ 1.35×10^{-1} s $^{-1}$. Note that the elongational stress is approaching steady state.

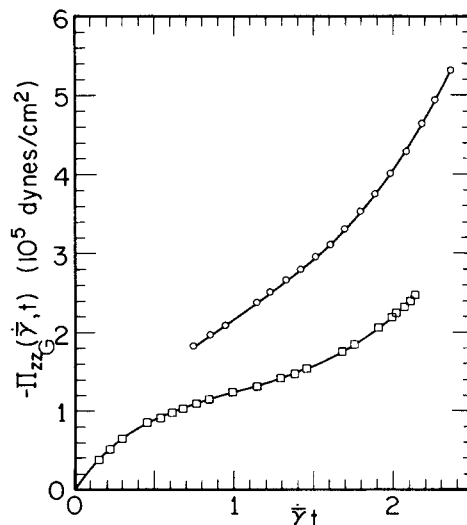


Fig. 6. Elongational stress versus strain for Natsyn 410 at 80°C. Symbols represent elongation rates as indicated: \square 6.37×10^{-4} s $^{-1}$; \circ 1.57×10^{-3} s $^{-1}$. Note that the elongational stress-strain curves are S-shaped.

These irregularities were judged to have a negligible effect on the steady state results.

If the elongational stress in Figures 4 and 5 were plotted as a function of time instead of strain, one would observe that with increasing elongation rate the elongational stress would attain steady state within a shorter time interval. This experimental result contradicts the predictions for elongational stress growth given by the rigid dumbbell model (15).

Additional details concerning these experimental results and elongational flow data for the isobutylene-isoprene copolymer at 80°C. have been given by Stevenson (13).

The experimental data described in this section are included in the summary of elongational flow data in Table I.

ACKNOWLEDGMENT

The author wishes to acknowledge the financial support of National Science Foundation Grant GP-1275 and fellowship support by the S. C. Johnson Company.

The guidance and inspiration provided by the author's research advisor, R. Byron Bird, is gratefully acknowledged. For many helpful suggestions during the course of this research, the author would like to thank Professor Arthur S. Lodge of the Engineering Mechanics Department, Professors Warren E. Stewart, Stuart L. Cooper, and James A. Koutsky of the Chemical Engineering Department, and Professor John D. Ferry of the Chemistry Department.

The author would also like to express his appreciation to Professor Warren C. Young of the Engineering Mechanics Department who made available a tensile testing machine and to Mr. John Dreger who ably operated this machine during elongational flow experiments. Everyone mentioned above is at the University of Wisconsin.

NOTATION

C_i	= capacitance connected across the i th amplifier
E	= output voltage from the analog computer
E_r	= relaxation modulus
E_0	= initial voltage for the analog computer
g	= acceleration due to gravity
II	= $\dot{\gamma}:\dot{\gamma}$, second invariant of the rate-of-strain tensor
L	= length of the monitored portion of the specimen at time t
L_i	= length of the monitored portion of the specimen after recovery
L_m	= maximum strained length of monitored portion of the specimen
L_0	= initial length of the monitored portion of the specimen
p	= pressure
r	= radial coordinate
R	= radius of monitored portion of specimen
R_i	= resistance connected to the i th amplifier
R_0	= initial radius of monitored portion of specimen
s	= $t - t'$
S	= interfacial tension
t	= present time
t'	= past time
t_1	= small time interval during which specimen is strained in instantaneous elongation experiment
z	= axial coordinate

Greek Letters

$\dot{\gamma}$	= shear rate
$\dot{\gamma}$	= $\frac{1}{2}(\nabla \mathbf{v} + (\nabla \mathbf{v})^T)$, rate-of-strain tensor
$\bar{\gamma}$	= total elongational strain
$\bar{\gamma}_e$	= elastic strain

$\bar{\gamma}_i$	= irrecoverable component of total elongational strain
$\bar{\gamma}_m$	= maximum total elongational strain
$\bar{\gamma}_r$	= recoverable component of total elongational strain
$\dot{\gamma}$	= elongation rate
$\dot{\gamma}^*$	= complex amplitude of $\dot{\gamma}$ in oscillatory elongational flow, assumed small
ϵ	= conventional strain
η	= steady shear viscosity
η^*	= complex shear viscosity
η_0	= zero-shear-rate shear viscosity
$\bar{\eta}$	= elongational viscosity
$\bar{\eta}^*$	= complex elongational viscosity
$\bar{\eta}'$	= real component of complex elongational viscosity
$\bar{\eta}''$	= imaginary component of complex elongational viscosity
$\bar{\eta}_0$	= zero-elongation-rate elongational viscosity
λ_1	= longest relaxation time for fluid
π_{rr}	= $p + \tau_{rr}$, radial component of total stress
π_{zz}	= $p + \tau_{zz}$, axial component of total stress
π_{zz0}	= axial component of total stress in a constant stress experiment
π_{zz}^0	= complex amplitude of π_{zz} in oscillatory elongational flow
ρ	= density of specimen
ρ_f	= density of fluid surrounding the specimen
τ_{rr}	= radial component of stress
τ_{zz}	= axial component of stress
ψ	= relaxation function
ω	= frequency

Subscripts

G	= time dependent value during stress growth
R	= time dependent value during stress relaxation

Superscripts

+	= designates boundary condition evaluated on the fluid side of the specimen-fluid boundary
-	= designates boundary condition evaluated on the specimen side of the specimen-fluid boundary
e	= designates stress that can be applied experimentally

LITERATURE CITED

1. Lodge, A. S., "Elastic Liquids," Academic Press, New York (1964).
2. Cogswell, F. N., *Rheol. Acta*, **8**, 187 (1969).
3. Tobolsky, A. V., "Properties and Structures of Polymers," Wiley, New York (1960).
4. Ballman, R. L., *Rheol. Acta*, **4**, 137 (1965).
5. Vinogradov, G. V., B. V. Radushkevich, and V. D. Fikhman, *J. Poly. Sci. A-2*, **8**, 1 (1970).
6. Radushkevich, B. V., V. D. Fikhman, and G. V. Vinogradov, *Mekh. Polimerov*, **2**, 343 (1968).
7. *Ibid.*, *Dokl. Akad. Nauk, SSSR*, **180**, 404 (1968).
8. Vinogradov, G. V., V. D. Fikhman, and B. V. Radushkevich, and A. Ya. Malkin, *J. Poly. Sci. A-2*, **8**, 657 (1970).
9. Meissner, J., *Rheol. Acta*, **8**, 78 (1969).
10. *Ibid.*, **10**, 230 (1971).
11. Cogswell, F. N., *Plastics Polymers*, **36**, 109 (1968).
12. Saylak, D., *Appl. Poly. Symp.*, **1**, 247 (1965).
13. Stevenson, J. F., Ph.D. dissertation, Univ. Wisconsin, Madison (1970).
14. Cox, W. P., and E. H. Merz, *Am. Soc. Test. Mater.*, **247**, 178 (1958).
15. Bird, R. B., H. R. Warner, Jr., and D. C. Evans, paper submitted to *Forsch. Hochpolymerforschung*.
16. Coleman, B. D., and W. Noll, *Phys. Fluids*, **5**, 840 (1962).
17. Bird, R. B., W. E. Stewart, and E. N. Lightfoot, "Transport Phenomena," Wiley, New York (1960).
18. Coleman, B. D., H. Markovitz, and W. Noll, "Viscometric

19. Bird, R. B., W. E. Stewart, E. N. Lightfoot, and T. W. Chapman, "Lectures in Transport Phenomena," Am. Inst. Chem. Engrs. Contin. Ed. Ser. 4 (1969).
20. Fredrickson, A. G., "Principles and Applications of Rheology," Prentice-Hall, Englewood Cliffs, N. J. (1964).

APPENDIX A. SOLUTION OF THE STRESS EQUATIONS OF MOTION FOR ELONGATIONAL FLOW

In this appendix the stress equations of motion are solved to determine the stresses which are necessary to elongate a cylindrical specimen at a constant elongation rate. The analysis neglects end effects, but includes body forces and interfacial tension. It is an extension of work done previously by Coleman and Noll (16).

The velocity profile is given by

$$v_z = \dot{\gamma} z \text{ and } v_r = -\frac{1}{2} \dot{\gamma} r \quad (\text{A1})$$

Equations (A1) are combined with the stress equations of motion (17) to give

$$-\frac{\partial}{\partial z} \pi_{zz} = \rho \dot{\gamma}^2 z + \rho g \quad (\text{A2})$$

$$-\frac{\partial}{\partial r} \pi_{rr} - \frac{(\tau_{rr} - \tau_{\theta\theta})}{r} = \frac{1}{4} \rho \dot{\gamma}^2 r \quad (\text{A3})$$

where ρ is the density of the specimen and g is the acceleration due to gravity. The direction of flow is opposite to the direction of gravitational acceleration. In steady elongational flow the $\tau_{rr} - \tau_{\theta\theta}$ term is zero for incompressible fluids in which the stress is determined by the strain history (16).

Equations (A2) and (A3) are then integrated and the integration constants are evaluated by the requirement that at steady state the difference $\pi_{zz} - \pi_{rr}$ is a function of the elongation rate alone. This requirement follows from the basic assumption for incompressible simple fluids that the stress is determined by the local strain history which, in this case, is determined by the elongation rate (1, 16, 18).

By this procedure we obtain

$$-\pi_{zz} = \frac{1}{2} \rho \dot{\gamma}^2 \left(z^2 + \frac{1}{4} r^2 \right) + \rho g z + f(\dot{\gamma}) + C \quad (\text{A4})$$

$$-\pi_{rr} = \frac{1}{2} \rho \dot{\gamma}^2 \left(z^2 + \frac{1}{4} r^2 \right) + \rho g z + C \quad (\text{A5})$$

The dependence on $\dot{\gamma}$ in Equation (A5) has been included in the pressure term p of the total stress π_{rr} .

Equation (A5) shows that an external radial normal stress of the form

$$\pi_{R+R+} = -\frac{1}{2} \rho \dot{\gamma}^2 \left(z^2 + \frac{1}{4} R^2 \right) - \rho g z \quad (\text{A6})$$

must be applied to the cylindrical boundary $r = R$ in order to maintain elongation at a constant elongation rate. The unknown constant C in Equations (A4) and (A5) is evaluated for the boundary condition

$$\pi_{R-R-} = \pi_{R+R+} + \frac{S}{R} \text{ at } r = R \quad (\text{A7})$$

where S is the interfacial tension. With this boundary condition, Equations (A4) and (A5) become

$$-\pi_{zz} = \rho g z + \frac{1}{2} \rho \dot{\gamma}^2 \left(z^2 + \frac{1}{4} r^2 \right) - \frac{S}{R} + f(\dot{\gamma}) \quad (\text{A8})$$

$$-\pi_{rr} = \rho g z + \frac{1}{2} \rho \dot{\gamma}^2 \left(z^2 + \frac{1}{4} r^2 \right) - \frac{S}{R} \quad (\text{A9})$$

where the terms in Equation (A8) represent the total stress and the gravitational, inertial, interfacial tension and viscoelastic contributions to the total stress, respectively.

In an actual elongation experiment, the only z -dependent external radial normal stress that can be applied to the cylindrical boundary is that due to hydrostatic pressure in the surrounding medium. This external radial normal stress is given by

$$\pi_{R+R+}^e = -\rho_f g z = \pi_{rr}^e \quad (\text{A10})$$

where ρ_f is the density of the fluid surrounding the specimen.

The maximum error $\Delta\pi_{RR}$ resulting from the inability to apply the proper external radial stress can be obtained by subtracting Equation (A10) from Equation (A9) evaluated at $r = R$ and $z = L_m$

$$-\Delta\pi_{RR} = (\rho - \rho_f) g L_m + \frac{1}{2} \rho \dot{\gamma}^2 \left(L_m^2 + \frac{1}{4} R^2 \right) - \frac{S}{R}$$

Error as a %	1.5%	10-10%	- 2.1%
	of $3\eta_0\dot{\gamma}$		

$$(\text{A11})$$

The numbers printed under Equation (A11) indicate the error for each term as a percentage of the "viscous" elongational stress $3\eta_0\dot{\gamma}$ for the following conditions: $\eta_0 = 10^7$ poise, $\dot{\gamma} = 2 \times 10^{-4} \text{ s}^{-1}$, $\dot{\gamma}_m = 1$, $S = 50$ dynes/cm, $L_0 = 5$ mm, $R_0 = 6.5$ mm, and $\rho - \rho_f = 0.0675 \text{ g/cm}^3$. From among conditions typical of the experiments with the isobutylene-isoprene copolymer, these conditions were chosen because they maximize the total absolute percentage error in the monitored portion of the specimen.

The effect of drag caused by the motion of the specimen relative to the surrounding fluid can be neglected because the ratio of the viscosity of the fluid to that of the specimen is on the order of 10^{-9} .

For the elongational flow experiments described in this paper, the maximum error in the stress $\Delta\pi_{RR}$ is small compared to the "viscous" elongational stress. The small magnitude of this error means that the stresses which can be applied experimentally are sufficient to stretch the specimen at an elongation rate that is very nearly constant along the length of the monitored portion of the specimen.

APPENDIX B. INTERRELATIONS OF ELONGATIONAL FLOW MATERIAL FUNCTIONS BASED ON THE THEORY OF LINEAR VISCOELASTICITY

Interrelations among material functions based on a simple constitutive equation should be a helpful guide for future experimental work and a useful check on rheological models under certain limiting conditions. A number of such interrelations for shear flow have been given by Bird (19). In this appendix several analogous interrelations are derived for elongational flow.

The constitutive equation obtained from the theory of linear viscoelasticity is ordinarily written (20)

$$\tau = -2 \int_{-\infty}^t \psi(t-t') \dot{\gamma}(t') dt' \quad (\text{B1})$$

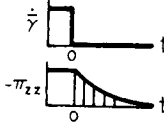
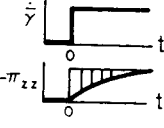
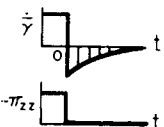
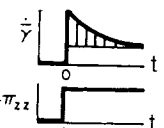
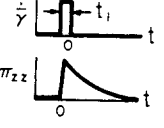
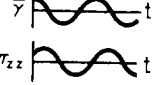
where τ is the stress tensor, $\psi(t-t')$ is the relaxation function and $\dot{\gamma}(t')$ is the rate-of-strain tensor.

As written above, Equation (B1) is not materially objective (18) but if it is written in convected coordinates and then transformed to space coordinates, a materially objective form of Equation (B1) is obtained (1, 18). This procedure may be carried out using a contravariant rate-of-strain tensor in convected coordinates and a relaxation function given by

$$\psi(t-t') = \frac{\eta_0}{\lambda_1} \exp(-(t-t')/\lambda_1) \quad (\text{B2})$$

For this case the material functions for steady elongational flow predicted by Equation (B1) approach the material func-

TABLE B1. SUMMARY OF ELONGATIONAL FLOW MATERIAL FUNCTIONS BASED ON THE THEORY OF LINEAR VISCOELASTICITY

Type of experiment	Elongation rate Elongational stress	Constitutive equation	Function equal to $\frac{\int_0^\infty \psi(s) s ds}{\int_0^\infty \psi(s) ds}$ where $s = t - t'$
Stress relaxation		$t < 0 \quad \pi_{zz}(\dot{\gamma}) = -3\dot{\gamma} \int_{-\infty}^t \psi(t-t') dt'$ $t > 0 \quad \pi_{zzR}(\dot{\gamma}, t) = -3\dot{\gamma} \int_{-\infty}^0 \psi(t-t') dt'$	$\frac{\int_0^\infty \pi_{zzR}(\dot{\gamma}, t) dt}{\pi_{zz}(\dot{\gamma})}$
Stress growth		steady state $\pi_{zz}(\dot{\gamma}) = -3\dot{\gamma} \int_{-\infty}^t \psi(t-t') dt'$ $t > 0 \quad \pi_{zzG}(\dot{\gamma}, t) = -3\dot{\gamma} \int_0^t \psi(t-t') dt'$	$\frac{\int_0^\infty (\pi_{zz}(\dot{\gamma}) - \pi_{zzG}(\dot{\gamma}, t)) dt}{\pi_{zz}(\dot{\gamma})}$
Recoverable strain		$t < 0 \quad \pi_{zz}(\dot{\gamma}) = -3\dot{\gamma} \int_{-\infty}^t \psi(t-t') dt'$ $t > 0 \quad \pi_{zz} = 0 = -3\dot{\gamma} \int_{-\infty}^0 \psi(t-t') dt'$ $-3 \int_0^t \psi(t-t') \dot{\gamma}(t') dt'$	$\frac{\dot{\gamma}_r}{\dot{\gamma}} = \frac{-\int_0^\infty \dot{\gamma}(t') dt'}{\dot{\gamma}}$
Elastic strain		steady state $\pi_{zz0}(\dot{\gamma}) = -3\dot{\gamma} \int_{-\infty}^t \psi(t-t') dt'$ $t > 0 \quad \pi_{zz0}(\dot{\gamma}) = -3 \int_0^t \psi(t-t') \dot{\gamma}(t') dt'$	$\frac{\bar{\gamma}_e}{\dot{\gamma}} = \frac{\int_0^\infty (\dot{\gamma}(t') - \dot{\gamma}) dt'}{\dot{\gamma}}$
Stress relaxation (inst. strain)		$t > 0 \quad \frac{-\pi_{zz}(t)}{\epsilon} = \lim_{t_1 \rightarrow 0} \frac{\int_0^{t_1} \psi(t-t') dt'}{t_1} = 3\psi(t) = E_r(t)$	$\frac{\int_0^\infty E_r(t) t dt}{\int_0^\infty E_r(t) dt}$
Small amplitude oscillatory elongation		$\dot{\gamma} = \text{Re} \{ \dot{\gamma}^0 \exp(i\omega t) \}$ $\bar{\eta}' - i\bar{\eta}'' = \frac{-\pi_{zz}^0}{\dot{\gamma}^0} = 3 \int_{-\infty}^t \psi(t-t') \exp(-i\omega(t-t')) dt'$ where Re is the real operator	$\lim_{\omega \rightarrow 0} \frac{\bar{\eta}''(\omega)}{\bar{\eta}'(\omega) \omega}$

tions predicted by the objective form of the constitutive equation in the limit as $(1 - 2\dot{\gamma}\lambda_1)(1 + \dot{\gamma}\lambda_1) \rightarrow 1$ or as $\epsilon \rightarrow 0$. Additional details of this calculation have been given by Stevenson (13).

Interrelations among various measurable material functions for elongational flow are given in Table B1. In addition to the material functions presented in the body of this paper, Table B1 includes material functions for elongational stress relaxation and small amplitude oscillatory elongation. All of the functions in the last column in Table B1 can be shown to be equal to $\int_0^\infty \psi(s) s ds / \int_0^\infty \psi(s) ds$.

As an example of the intermediate steps for the calculations summarized in Table B1, the results for the recoverable strain are worked out below. In a recoil experiment, the steady state elongation rate $\dot{\gamma}$ is constant for $-\infty < t < 0$. At $t = 0$ the elongational stress $\pi_{zz} = (\tau_{zz} - \tau_{rr})$ is instantly removed and the specimen recoils with elongation rate $\dot{\gamma}(t)$ for $t > 0$. The recoverable elongational strain is given by

$$-\dot{\gamma}_r = \int_0^\infty \dot{\gamma}(t') dt' \quad (\text{B3})$$

For this experiment Equation (B1) assumes the form

$$t > 0, \quad \pi_{zz} = 0 = -3 \int_{-\infty}^0 \psi(t-t') \dot{\gamma} dt'$$

$$-3 \int_0^t \psi(t-t') \dot{\gamma}(t') dt' \quad (\text{B4})$$

or

$$-\dot{\gamma} \int_{-\infty}^t \psi(s) ds = \int_0^t \psi(s) \dot{\gamma}(t-s) ds \quad (\text{B5})$$

where $s = t - t'$. Equation (B5) is integrated from 0 to ∞ over t and the order of integration is changed to give

$$-\dot{\gamma} \int_0^\infty \psi(s) s ds = \int_0^\infty \psi(s) \left[\int_0^\infty \dot{\gamma}(t') dt' \right] ds \quad (\text{B6})$$

where the term in square brackets $[]$ is $-\dot{\gamma}_r$. Equation (B6) can be rearranged to

$$\frac{\dot{\gamma}_r}{\dot{\gamma}} = \frac{\int_0^\infty \psi(s) s ds}{\int_0^\infty \psi(s) ds} \quad (\text{B7})$$

which is the result reported in the last column in Table B1 for recoverable strain.

Manuscript received September 24, 1971; paper accepted November 8, 1971.